ELEMENTA
Science of the Anthropocene

Diurnal cycle of ozone throughout the troposphere over Frankfurt as measured by MOZAIC-IAGOS commercial aircraft

H. Petetin[1*] • V. Thouret[1] • G. Athier[1] • R. Blot[1] • D. Boulanger[2] • J.-M. Cousin[1] • A. Gaudel[3,4] • P. Nédélec[1] • O. Cooper[3,4]

[1]Laboratoire d'Aérologie, Université de Toulouse, CNRS, UPS, France
[2]Observatoire Midi-Pyrénées, Université de Toulouse, CNRS, UPS, France
[3]Cooperative Institute for Research in Environmental Sciences, University of Colorado, Boulder, Colorado, United States
[4]NOAA Earth System Research Laboratory, Boulder, Colorado, United States
[*]hervepetetin@gmail.com

Abstract

Ozone is generally assumed to have weak diurnal variations in the free troposphere due to lower production rates than in the boundary layer, in addition to a much lower NO titration and the absence of dry deposition at the surface. However, this hypothesis has not been proven due to a lack of high frequency observations at multiple times per day. For the first time, we take benefit from the frequent O_3 vertical profiles measured above Frankfurt in the framework of the MOZAIC-IAGOS program to investigate the diurnal variations of O_3 mixing ratios at multiple pressure levels throughout the troposphere. With about 21,000 aircraft profiles between 1994 and 2012 (98 per month on average), distributed throughout the day, this is the only dataset that can allow such a study. As expected, strong diurnal variations are observed close to the surface, in particular during spring and summer (enhanced photochemistry and surface deposition). Higher in altitude, our observations show a decrease of the diurnal cycle, with no diurnal cycle discernible above 750 hPa, whatever the season. Similar results are observed for the different percentiles of the O_3 distribution (5^{th}, 25^{th}, 50^{th}, 75^{th}, 95^{th}). An insight of the changes of the diurnal cycles between 1994–2003 and 2004–2012 is also given. We found higher O_3 mixing ratios during the latter period, particularly on the lowest pressure levels, despite lower mixing ratios during summer.

Domain Editor-in-Chief
Detlev Helmig,
University of Colorado Boulder

Associate Editor
Samuel J. Oltmans,
CIRES, University of Colorado

Knowledge Domain
Atmospheric Science

Article Type
Research Article

Part of an *Elementa* Special Feature
Reactive Gases in the Global Atmosphere

Received: May 12, 2016
Accepted: August 31, 2016
Published: September 30, 2016

1. Introduction

Ozone (O_3) is a trace gas of major importance in the atmosphere due to its adverse effects on health, vegetation and climate change. In the troposphere, O_3 is produced photochemically by the oxidation of methane, carbon monoxide (CO) and non-methane hydrocarbons (NMHCs) in the presence of nitrogen oxides (NO_x=NO+NO_2) and sunlight, or transported downward from the stratosphere. It is removed by dry deposition, titration by NO and reactions with hydrogen oxide radicals (HO_x=OH+HO_2) (Monks, 2005). Ozone is lost in low-NO_x environments, such as the marine boundary layer. Halogens also play a role in the ozone chemistry, directly through a reaction with O_3 itself, or indirectly through a reaction with NMHCs (production or destruction of O_3 depending on the conditions) (Monks et al., 2015).

During the last several decades, numerous studies have investigated the causes and characteristics of the diurnal variation of surface O_3 at a wide range of locations (Singh et al., 1978; Oltmans and Levy, 1994; Pryor and Steyn, 1995; Zhang et al., 2004). At low altitudes over continental regions under the influence of anthropogenic emissions, ozone generally exhibits minimum mixing ratios during night, mainly due to dry deposition and titration by NO in the shallow nocturnal boundary layer (BL). During daytime, mixing ratios increase under the combined effect of photochemical production and mixing with O_3-rich air masses from the residual BL, reaching a maximum in the afternoon. The diurnal cycle typically has its maximum

amplitude in summer when photolysis rates are the highest, while diurnal cycles observed in winter are less pronounced. Over regions with a more complex orography, the local dynamics can play a more important, if not dominant, role in the diurnal variability of O_3. At high-altitude mountain sites, observations usually show a reverse cycle, with maximum mixing ratios during night (e.g. Bonasoni et al., 2000; Cristofanelli et al., 2013; Ezcurra et al., 2013; Zhang et al., 2015). This pattern is the result of the mountain peaks being heavily influenced by the lower free troposphere at night where ozone mixing ratios are typically greater than at the surface if the mountain is located in a rural or remote region. During the day upslope flow caused by the heating of the mountain slopes brings ozone depleted air from the BL up to the summit (Oltmans and Komhyr, 1986; Oltmans et al., 2013). In the marine BL, daytime O_3 can be destroyed by photolysis, reactions with HO_x and halogens or dry deposition (Ganzeveld et al., 2009). During summertime, when low-NO_x conditions prevail over oceans, these sinks dominate the O_3 production by photolysis of NO_2 and the entrainment from aloft in the free troposphere (FT) usually leading to minimum mixing ratios in the afternoon (Ayers et al., 1992; Monks et al., 1998, 2000).

As investigating the O_3 diurnal variability requires a sufficiently high frequency of measurements (typically 1h), all the previous studies have been restricted to the surface. In the FT, neither satellite observations nor ozone soundings are frequent enough to derive a complete diurnal profile of O_3. In principle, Lidar measurements over a sufficiently long period may be used to investigate the diurnal cycle of O_3 at multiple levels in the troposphere (although with more uncertainties than considering in-situ observations) but to our knowledge, no such studies exist (probably because such Lidar observations are complex to operate routinely during long periods). The changes of diurnal variability with altitude have been investigated during some campaigns with several instruments deployed at different altitudes along a mountain slope, showing a decrease of the O_3 diurnal variability with altitude, and a slight reverse at the highest elevations with greater mixing ratios during night (Ezcurra et al., 2013; Burley et al., 2015; Brodin et al., 2010). However, the previously mentioned strong influence of the local dynamics in such environments prevents extrapolation of these results to the FT.

Airborne observations of O_3 (among other species) have been measured by the MOZAIC-IAGOS program since 1994 using commercial aircraft from several airlines. Vertical profiles from the surface to 11–12 km are obtained as the aircraft operationally descend and ascend from airports. Among the 200 airports visited worldwide, the Frankfurt, Germany airport is by far the most frequently visited, with approximately 21,600 flights between 1994 and 2012, which corresponds to 98 flights per month, on average. During this long period, airline schedules have varied enough to have yielded observations that are reasonably well-distributed throughout the day. In this paper, we take advantage of these high-frequency measurements to investigate the diurnal variations of O_3 throughout most of the troposphere (0–12 km).

The observational dataset is described in Sect. 2. Section 3 presents the results, including the diurnal profiles of O_3 in the troposphere and their change over the last two decades. Results are discussed in Sect. 4.

2. Dataset and methods

2.1 MOZAIC-IAGOS observations

The MOZAIC (Measurements of OZone and water vapour on Airbus In-service airCraft) program, initiated in 1994 and incorporated into the IAGOS (In-service Aircraft for a Global Observing System; www.iagos.org) program since 2011 takes advantage of commercial aircraft to provide worldwide in-situ measurements of several trace gases (e.g., O_3, CO) and meteorological parameters (e.g. water vapour) throughout the troposphere and the lower stratosphere (Marenco et al., 1998; Petzold et al., 2015; Nédélec et al., 2015). Ozone measurements are performed using a dual-beam UV-absorption monitor (time resolution of 4 seconds) with an accuracy of ±(2 ppbv+2%) (Thouret et al., 1998). More details on the new IAGOS instrumentation can be found in Nédélec et al. (2015). The continuity of the dataset between the MOZAIC and IAGOS programs has been demonstrated based on the 2-year overlap (2011–2012) (Nédélec et al., 2015).

In this study, we focus on the vertical profiles above the Frankfurt airport where observations are the most frequent. The coverage and density of the datasets are described in Sect. 2.3. Note that the availability of observations at different times of day is due to several MOZAIC-IAGOS aircraft simultaneously serving this destination. Some other airports have also been frequently visited by MOZAIZ-IAGOS aircraft (e.g. New York, Paris, Windhoek, Vienna, Tokyo), but usually by only one aircraft during specific time frames, resulting in too few profiles to properly investigate the diurnal variations of O_3.

2.2 Data treatment

During landing and take-off phases, observations are obtained through most or all of the troposphere, and often part of the lower stratosphere. The time resolution of 4 seconds roughly corresponds to a vertical distance of 30 m. As landing and take-off do not exactly correspond to vertical profiles, only the observations within the 400 km around the Frankfurt airport are considered, which limits the possible spread of O_3 mixing ratios due to horizontal heterogeneity. This study focuses on tropospheric O_3, and observations at the tropopause level and in the stratosphere are thus ignored. However, stratospheric intrusions within the

troposphere are retained (i.e. vertical profiles are not purely tropospheric). Here, the tropopause is defined as the 30 hPa-width layer centred on the 2 pvu (potential vorticity units) iso-surface, following the method of Thouret et al. (2006). The PV values are extracted along each vertical profile from the European Centre for Medium-Range Weather Forecasts (ECMWF) operational analysis (00:00, 06:00, 12:00, 18:00 UTC) and forecasts (03:00, 09:00, 15:00, 21:00 UTC). More details on the procedure are given in Petetin et al. (2015).

Data are aggregated on 50-hPa pressure surfaces from 1000 to 300 hPa. For the construction of the diurnal profile, we consider time intervals of 3 hours: 0–3, 3–6, 6–9, 9–12, 12–15, 15–18, 18–21, 21–24 UTC. For convenience, hours in this paper are expressed in UTC; note that in Germany, the local solar time (LST) corresponds to UTC+1 from November to March (included), and UTC+2 otherwise (the 0–3 UTC time interval thus roughly corresponds to the closing times of the airport). Diurnal profiles are calculated at both the seasonal (DJF: December-February, MAM: March-May, JJA: June-August, SON: September-November) and annual scale (ANN: annual). Note that observations are far too sparse during the 0–3 UTC time interval and are therefore ignored in this paper. The procedure is applied to several metrics, including the mean and 5^{th}, 25^{th}, 50^{th}, 75^{th} and 95^{th} percentiles.

2.3 Density and coverage of the dataset

The number of O_3 observations available over the 1994–2012 period for the calculation of the diurnal cycles is reported in Table S1 in the Supplement. On average, each point of the diurnal cycle (corresponding to a given 3-hour time interval and a given 50-hPa pressure level) relies on about 52,000 observations. However, this density strongly varies depending on the time of day. The densest sampling is available between 3 and 12 UTC (above 80,000 observations), followed by 12–15 UTC (around 54,000) and 15–18 UTC (around 29,000). A substantially lower density occurs between 18 and 24 UTC (below 16,000 observations). The sampling is reasonably well balanced between the different seasons, with 29, 22, 29 and 20% of the data obtained in winter, spring, summer and autumn, respectively.

In terms of spatial coverage, observations available before 18 UTC are mostly obtained from flight routes north of Frankfurt, while observations after 18 UTC are typically south of Frankfurt. Considering that (i) the tropopause height decreases as one moves northward and that (ii) there are some uncertainties associated with the estimation of PV, this sampling bias may result in more frequent occurrences of stratospheric contamination before 18 UTC than after. However, due to the fact that only the troposphere is considered in this study and that we take into account only the observations within 400 km of the Frankfurt airport, this source of uncertainty is expected to be low.

It is worth noting that some uncertainties may arise from the temporal discontinuity of this database. Indeed, measurements are not performed continuously throughout the day (as occurs at a surface station), but sporadically between 1994 and 2012 with frequencies that vary from one 3-hour time interval to another. The data coverage at 800 hPa is shown in Fig. 1 for the different time intervals. Between 3 and 15 UTC, observations are available during almost all the 1994–2012 period. At 15–18 UTC, observations are sparse between 2005 and 2010 (inclusive). The least dense coverage concerns the 18–21 UTC time interval, and to a lesser extent the 21–24 UTC. Considering the strong inter-annual variability (IAV) of O_3 (Thouret et al., 2006; Zbinden et al., 2006), this may introduce some variability unrelated to the diurnal cycle. For instance, at 800 hPa, contrary to the other time intervals, no observations are available at 18–21 UTC during the summer 2003 when a severe heat wave induced a strong positive O_3 anomaly over Europe, mostly in the BL (Solberg et al., 2008; Tressol et al., 2008; Ordóñez et al., 2005). The absence of MOZAIC-IAGOS observations during that season thus produced a low O_3 bias. Depending on the extent of this bias, it may lead to an artificial diurnal variation.

In order to assess the potential importance of this bias, sensitivity tests were performed based on continuous O_3 measurements at the surface in the region of Frankfurt. We considered 3 stations of the German Federal Environment Agency (Umweltbundesamtes, UBA) – the Rannheim (50.01°N, 8.45°E, 90 m; station code DEHE018; located 5 km westward from the Frankfurt airport) and Darmstadt (49.97°N, 8.66°E, 158 m; DEHE001; 12 km southward) urban background stations, and the Spessart regional background station (50.16°0N, 9.40°E, 502 m; DEHE026; 50 km eastward) – as well as the Waldhof (52.80°N, 10.77°E, 74 m; 300 km north-eastward) regional background station from the Global Atmosphere Watch (GAW) network. For each of these surface stations, hourly observations of O_3 are available continuously from October 1994

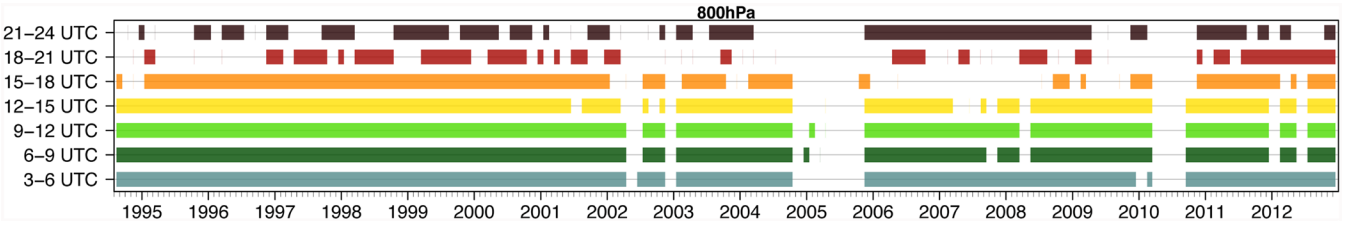

Figure 1

Data coverage on a monthly basis at 800 hPa for the different 3-hour time intervals.

For each time interval (associated to its own colour for clarity), months with at least one observation in the pressure layer centred around 800 hPa are coloured, while blanks indicate the absence of observations. For instance, during the 3–6 UTC time interval, observations are available all along the 1994–2012 period, except during a large part of 2005 and 2010 as well as during a few months in 2003–2004. The coverage is similar at 6–9, 9–12 and 12–15 UTC, while data are the sparsest at 18–21 UTC.

doi: 10.12952/journal.elementa.000129.f001

to December 2012. The seasonal and annual diurnal cycles are then calculated over 3-hour time intervals (as explained in Sect. 2.2) using this surface O_3 dataset, but with three different types of data selection. First, as a reference case, we use all the available data between 1994 and 2012 (hereafter referred as REF). Second, we consider only the months with at least 1 observation available at 1000 hPa at the corresponding 3-hour time interval in the Frankfurt MOZAIC-IAGOS database (hereafter referred as SUB1). Third, similarly to SUB1, we consider only the months with at least 50 observations available at 1000 hPa n the Frankfurt MOZAIC-IAGOS database (hereafter referred as SUB50). In both the SUB1 and SUB50 cases, we thus artificially create the same data gaps present in the MOZAIC-IAGOS dataset in our surface O_3 dataset. Comparing the REF diurnal cycles with the SUB1 and SUB50 allows us to quantify the bias introduced by the absence of observations during some periods. Results are shown in Fig. S1 in the Supplement. Whatever the season and the station, the differences of 3-hour mean mixing ratios between the REF and SUB1 (SUB50) diurnal cycles remain below ±3% (±13%). They are usually greatest at 18–21 UTC, when the MOZAIC-IAGOS data coverage is sparsest. These low differences demonstrate that the data gaps in the MOZAIC-IAGOS dataset likely have a limited impact on the diurnal cycles calculated at Frankfurt, at least close to the surface where these stations are expected to be reasonably well representative (in particular the rural background ones). Similar results are obtained when considering the data coverage of MOZAIC-IAGOS at the other pressure levels. However, it is worth noting that at altitude, these surface observations cannot be considered to be representative.

3. Results

3.1 Diurnal profile of mean tropospheric O_3

The diurnal profiles of mean tropospheric O_3 over the 1994–2012 period are shown in Fig. 2 at both the seasonal and annual scale. Note that compared to the uncertainty associated with each individual measurement (estimated at ±(2 ppb+2%), see Sect. 2.1), the uncertainties associated with the mean O_3 mixing ratios are largely reduced due to the large number of points (see Table S1 in the Supplement), all values remaining below 0.1 ppb.

As expected, the strongest diurnal variations occur in the BL due to the more active O_3 production and loss processes close to the surface. The BL diurnal cycle reaches its highest amplitude in summer (25 ppb at 1000 hPa) when the photochemical production is at a maximum, followed by spring (17 ppb) and autumn (12 ppb), while very low variations are observed in winter (4 ppb). The diurnal variation propagates higher in altitude in summer due to the development of a deeper convective BL. In particular, the O_3 maximum at 15–18 UTC extends to all pressure levels up to 800 hPa. At 1000 hPa and to a lesser extent at 950 hPa, mixing ratios quickly decrease after 18 UTC, down to 20 ppb at 3–6 UTC, close to the surface. This is likely due to the combined effect of dry deposition and titration by NO (both sinks being enhanced in the shallow nocturnal BL), as suggested by the much lower decrease in the next level. In the early morning (6–9 UTC), the O_3 vertical gradient between 1000 and 950 hPa is slightly reduced compared to the night. This is likely due to the turbulence that starts to mix low-O_3 air masses from the nocturnal BL with high-O_3 air masses from the residual BL (Zhang and Rao, 1999). Later, this O_3 vertical gradient keeps decreasing as the turbulent mixing increases, which progressively homogenizes the O_3 mixing ratios in the BL.

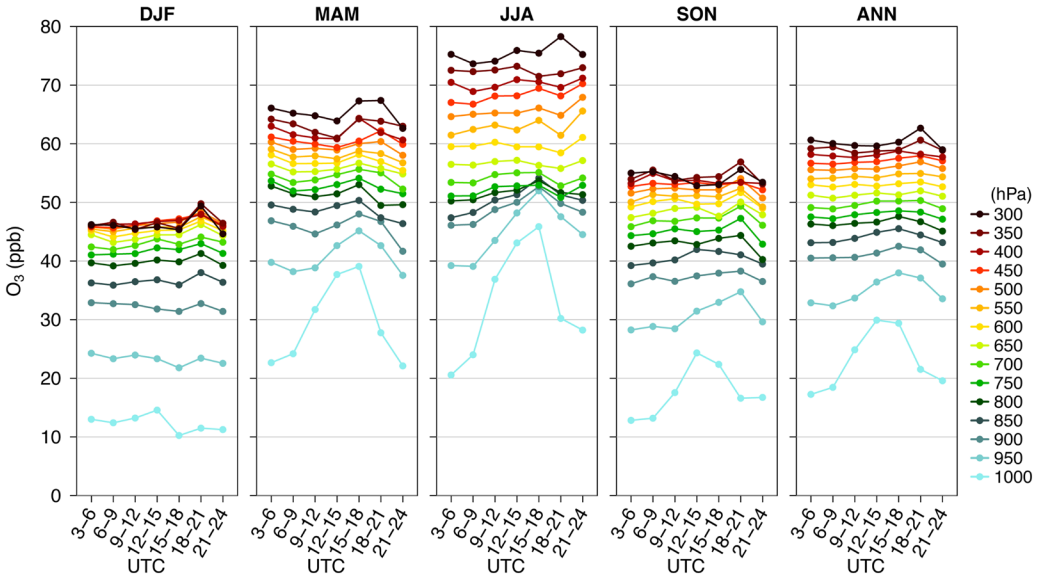

Figure 2

Diurnal variations of the mean O_3 mixing ratios in the troposphere above Frankfurt.

The diurnal variations of the mean O_3 mixing ratios are calculated by aggregating all the observations obtained above Frankfurt between 1994 and 2012. Results are shown at 15 pressure level in the troposphere, at both the seasonal and annual scale (DJF: winter, MAM: spring, JJA: summer, SON: autumn, ANN: annual). Diurnal variations appear strong in the first levels, but quickly decrease higher in altitude.

doi: 10.12952/journal.elementa.000129.f002

Higher in altitude, there is an absence of strong O_3 diurnal variations, regardless of season. Some variations are still observed at some pressure levels after 18 UTC, and in particular an increase at 18–21 UTC above 350 hPa. This may be an artefact related to the sparser observations at this time of day. Interestingly, based on the observations at the Waldhof station, we previously highlighted (in Sect. 2.3) that this lower frequency of measurement may introduce a moderate positive bias in the diurnal cycle at 18–21 UTC. However, it is not possible to draw definitive conclusions on this point since this bias was mainly observed during the winter and is likely limited to the lower troposphere (i.e. the representativeness of the Waldhof surface station). In any event, coefficients of variation (CV) – defined as the standard deviation of the diurnal cycle normalized by its mean – quickly decrease from 10–30% at 1000 hPa to less than 4% above 950 hPa in winter, 850 hPa in spring, 800 hPa in summer and 900 hPa in autumn. Above 800 hPa, CV range between 0.6 and 3.3%. The highest values are found during the winter at the uppermost pressure levels while most of the CV values elsewhere remain around 1–2%.

Although small in amplitude, these diurnal variations in the free troposphere may still be statistically significant. For each season and each pressure level, between each pair of points of the diurnal cycle (21 possible combinations among the 7 time intervals), a Smith/Welch/Satterthwaite (SWS) t-test (Smith, 1936; Welch, 1938; Satterthwaite, 1946) (also referred as the unequal variance t-test in the literature) is performed to compare the mean O_3 mixing ratios. Ruxton (2006) explained why this SWS t-test should always be used in preference to the Student's t-test or Mann-Whitney U test (in particular, it does not assume equal variances between the two populations). Results indicate that most of the differences are statistically significant at a 95% confidence level. On average over all the pressure levels and 3-hour time intervals, about 85, 87, 79, 81 and 74% of the SWS t-tests performed gives significant differences in the DJF, MAM, JJA, SON and ANN diurnal cycles, respectively. This proportion of statistically different mixing ratios varies with altitude, from about 90–95% below 950 hPa to 72–78% around 650–350 hPa. Therefore, throughout the whole troposphere, most of the diurnal variations of O_3 mixing ratios are statistically significant, but both the relative amplitude of these variations and the proportion of significant differences are reduced higher in altitude.

3.2 Diurnal profile of the distribution of tropospheric O_3 mixing ratios

The diurnal profiles of the O_3 5th, 25th, 50th, 75th and 95th percentiles at the annual scale are shown in Fig. 3. As for the mean O_3 mixing ratios, strong diurnal variations are observed at the lowest levels but quickly decrease with altitude. Qualitatively, a similar picture emerges at the seasonal scale, although variations are usually higher (see Fig. S2–S5 in the Supplement). This is particularly true in summer for the O_3 95th percentile (Fig. 4), for which the mixing ratios at 21–24 UTC are 5–15 ppb higher than during the rest of the day at several pressure levels in the FT (600–300 hPa). However, the corresponding CVs remain below 6%.

Whatever the season or the metric, most of the O_3 vertical gradients – defined as positive when O_3 increases with altitude – in the troposphere are positive or only slightly negative. However, as illustrated in Fig. 4, a noticeable exception is the O_3 95th percentile in summer. During the afternoon, the vertical gradients are -0.22 ppb hPa^{-1} between 850 and 800 hPa (i.e. likely within the BL). At this time of year and day, the solar radiation reaches its maximum and is expected to enhance both the vertical transport and the photolysis rates. These negative gradients may thus suggest that the photochemical production of O_3 is faster than the vertical mixing.

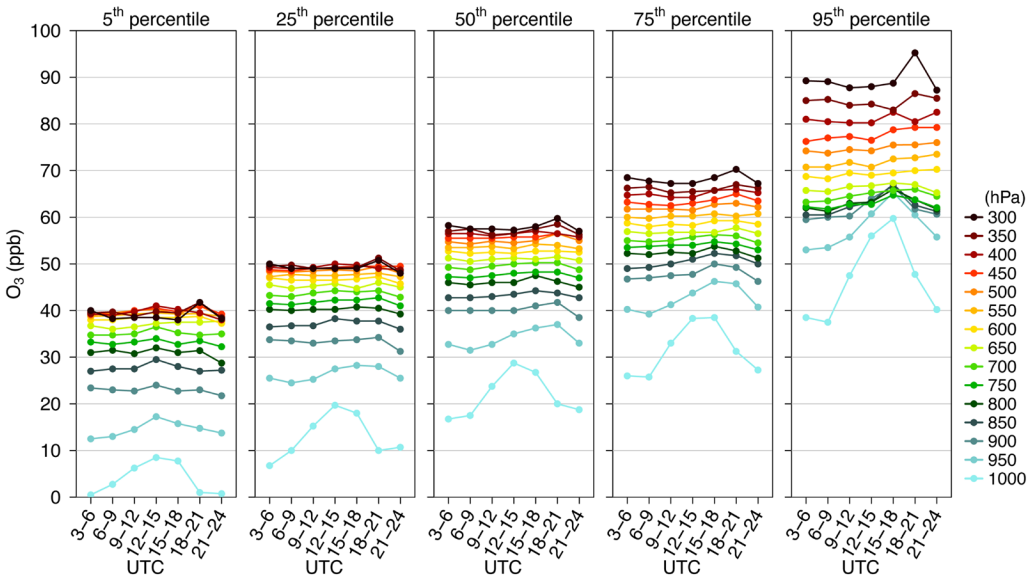

Figure 3

Diurnal variations of several O_3 percentiles in the troposphere above Frankfurt.

Results are shown for the O_3 5th, 25th, 50th, 75th and 95th percentiles, at the annual scale. As for the mean O_3 mixing ratios, diurnal variations are strong in the first levels but greatly reduced higher in altitude.

doi: 10.12952/journal.elementa.000129.f003

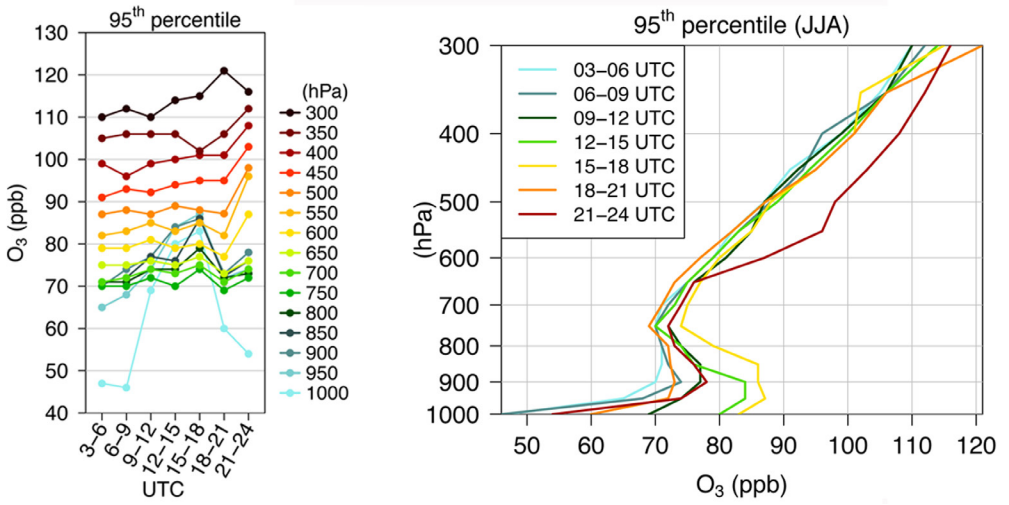

Figure 4

Diurnal variations of the O_3 95th percentile in summer.

The diurnal variations of the O_3 95th percentile in summer are shown on the left panel. The corresponding vertical profiles are shown on the right panel. A substantial enhancement of the O_3 mixing ratios is observed below 800 hPa during the middle of the day, leading to a strong negative gradient between 850 and 750 hPa.

doi: 10.12952/journal.elementa.000129.f004

3.3 Changes of the diurnal profile over the two past decades

We now investigate how the O_3 diurnal profile has changed over the past two decades. The dataset is split into two periods, 1994–2003 and 2004–2012. Fig. 5 shows the diurnal profiles of mean O_3 at the annual scale for both periods, and the relative differences between them (the difference being normalized by the mixing ratios observed during the first period). Note that in this section, we investigate only the changes of O_3, not the trends for which uncertainties would have to be estimated. Overall, the mean O_3 mixing ratios have slightly increased in most of the troposphere and during most of the day. The highest increases are found during the night close to the surface (changes between +21 and +41%). The much lower increase between 9 and 18 UTC (< +7%) leads to a strong decrease of the amplitude of the diurnal cycle, from 15 to 10 ppb. These changes quickly attenuate with altitude, the increase at 950 hPa remaining below +7%. In the second part of the day (after 15 UTC), a slight decrease of the O_3 mixing ratios is observed at some pressure levels, with values ranging between -3 and -1%.

Results at the seasonal scale (Fig. S6–S9 in the Supplement) indicate that the increase of night-time O_3 is observed during all seasons, at least at the first pressure level. It is more accentuated in winter/autumn (from +27 to +95%) than in spring/summer (from +3 to +28%). This increase is likely mainly due to the reduction of NO_x emissions in Europe over the last decades, leading to a lower titration of O_3 by NO (Derwent et al., 2003; Solberg et al., 2005; Jonson et al., 2006). In fact, the wintertime O_3 has increased in the whole troposphere and during the whole day, although at very different extents (from +1 to +20% above the 950-hPa pressure level). A similar picture emerges in spring, although with lower changes. Conversely, the increase in autumn appears confined to the BL (below the 600-hPa pressure level) and is observed throughout the

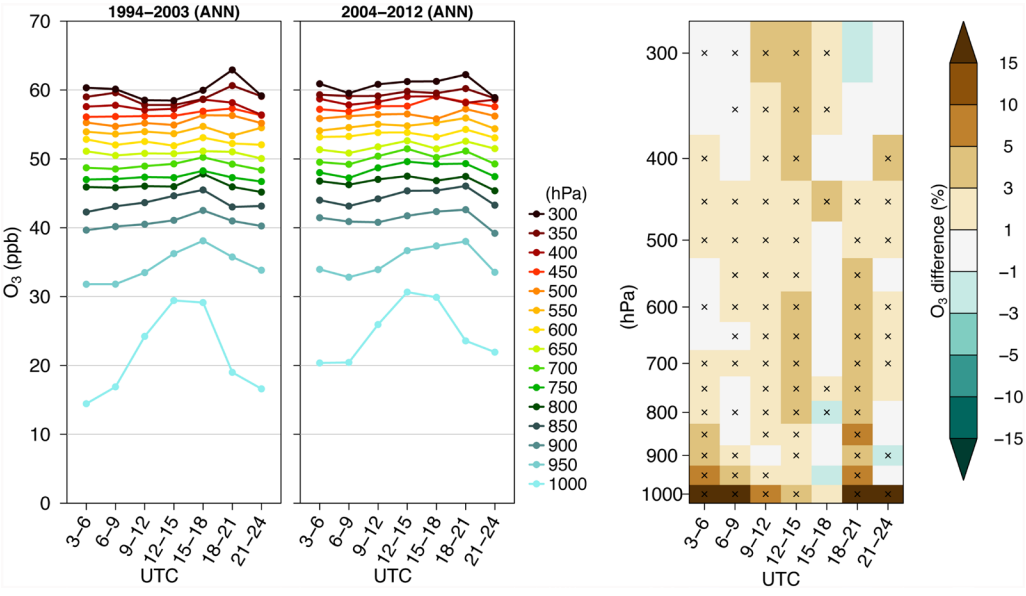

Figure 5

Changes of the diurnal variations of O_3 mixing ratios between 1994–2003 and 2004–2012.

Diurnal profiles of mean tropospheric O_3 mixing ratios are given for 1994–2003 (left panel) and 2004–2012 (middle panel). The relative differences of mixing ratio between the two periods are shown in the right panel. Crosses indicate the pressure levels and time interval at which the differences are statistically significant regarding the SWS t-test (see text in Sect. 3.1 for details on this test). The mean O_3 mixing ratios in 2004–2012 appear stronger than in 1994–2003 at most pressure levels and during most of the day, although all the differences are not significant regarding the SWS t-test. The largest increases (above +15%) are observed in the first levels during the night.

doi: 10.12952/journal.elementa.000129.f005

day except at 15–18 UTC where mixing ratios have decreased (from -3 to -9% above the 950-hPa pressure level). Contrary to the other seasons, the O_3 mixing ratios have decreased during summer (apart from the night-time increase at 1000 hPa), in particular below the 700-hPa pressure level where changes from 1994–2003 to 2004–2012 range between -16 and -2%. Above, the decrease is observed only after 18 UTC, although not at all pressure levels. This decrease of summertime O_3 in the BL during daytime partly compensates the increase observed during the other seasons.

The changes of the 5th and 95th percentiles at the annual scale are given in Fig. S10–S11 in the Supplement. Interestingly, the relative increase of the 5th percentile is substantially higher than for the mean O_3 (in particular close to the surface), while the 95th percentile is shown to decrease in large parts of the troposphere.

4. Discussion and conclusion

The diurnal variations of O_3 mixing ratios are well characterized at the surface in many different environments (e.g. urban, coastal, mountain, marine). However, due to the absence of continuous measurements at higher altitudes, both in the boundary layer and the FT, our knowledge of the O_3 diurnal variations relies on assumptions and/or numerical simulations. One generally assumes that O_3 mixing ratios in the free troposphere remain relatively constant throughout the day (in comparison to the surface). This assumption relies on the fact that the O_3 production rates are expected to be lower at altitude. In the free troposphere, a major part of the NO_x is tied up as peroxyacyl nitrate (PAN) where it is stable at cold temperatures (Singh et al., 1990; Ridley et al., 1990). Besides narrow plumes of lightning NO_x in which mixing ratios can reach several ppbv, NO_x mixing ratios remain low, typically ranging between 10 and 1000 pptv (Emmons et al., 1997; Huntrieser et al., 1998; Brunner et al., 2001; Cooper et al., 2006). Over central-western Europe, the NO_x mixing ratios measured close to thunderstorms in summer were mostly below 150 pptv at 3–8 km and below 400 pptv at 8–11 km (Huntrieser et al., 2002). As highly reactive hydrocarbons also have relatively low mixing ratios in the free and upper troposphere (Singh et al., 2000; Balzani Lööv et al., 2008; Helmig et al., 2008), a larger portion of the O_3 production (or consumption depending on the NO_x mixing ratio) relies on the slower oxidation of CO or CH_4. Using the GEOS-Chem model, Zhang et al. (2009) showed O_3 production rates of only about 1 ppbv day^{-1} in pollution plumes crossing the North Pacific in the FT. Even above the south-eastern United States where a large amount of lightning NO_x is available in summer, Cooper et al. (2006) reported O_3 production rates of only 3–4 ppbv day^{-1} in upper troposphere.

However, several O_3 sources including lightning NO_x and stratospheric intrusions may introduce some diurnal variability in the free and upper troposphere. The lightning NO_x emissions represent only 10% (4%) of the total NO_x emissions at the global scale (at northern midlatitudes) (Schumann and Huntrieser, 2007), but are known to contribute substantially to the formation of O_3 in the FT (DeCaria et al., 2005; Cooper et al., 2006, 2007, 2009). At midlatitudes above continents, a large part of these emissions occur in the middle and upper troposphere (Ott et al., 2010). Based on a lightning detection network of 30 antennas in Germany, Wapler (2013) highlighted a strong diurnal variation of the lightning activity, with a frequency of occurrence peaking at 14–18 UTC (whatever the season). Concerning troposphere-stratosphere exchange, to our knowledge, no previous study has investigated the existence of diurnal variations. However, during the Deep Convective Clouds and Chemistry (DC3) experiment (central United States, summer 2012), Pan et al. (2014) recently reported downward transport of stratospheric O_3-rich air masses in the vicinity of overshooting mesoscale convective systems. The thunderstorm activity is generally higher in the afternoon. Based on observations over Europe from the Spinning Enhanced Visible and Infrared Imager (SEVIRI) instrument aboard the Meteosat satellites, Bedka (2011) showed that over land, the frequency of occurrence of these overshooting cloud tops strongly varies throughout the day, with a maximum around 14–17 UTC. As for the formation of O_3 from lightning NO_x, this source may thus increase the O_3 mixing ratios during the late afternoon.

Based on the frequent profiles of MOZAIC-IAGOS aircraft above Frankfurt since 1994, the diurnal variations of the mean O_3 mixing ratios appear statistically significant regardless of pressure level. However, we demonstrate that these diurnal variations quickly decrease with altitude in the troposphere, and remain small in the middle and upper troposphere. Besides the fact that the photochemically-driven diurnal cycle of O_3 in the BL extends higher in altitude during the summer, we show that these low diurnal variations in the free and upper troposphere are observed regardless of season. Similar results are obtained for the different percentiles (5th, 25th, 50th, 75th, 95th) of the O_3 distribution.

Comparing the diurnal cycles between 1994–2003 and 2004–2012, we found an increase of O_3 in most of the troposphere and during most of the day. This change appears stronger close to the surface during the night, which leads to a decrease of the amplitude of the diurnal cycle in the BL. At the seasonal scale, this increase occurs mainly in winter, and to a lesser extent in spring and autumn while O_3 is shown to decrease during the summer, although only in the BL. Such changes are consistent with the shift of the O_3 seasonal cycle toward earlier maxima recently reported at several surface stations over Europe (Parrish et al., 2013) and observed mainly in the lower troposphere around Frankfurt (Petetin et al., 2015).

This result applies to central/western Europe but may be different at other locations, for instance in the inter-tropical convergence zone (ITCZ) where the deep convection is stronger and more frequent. While no other location has the high sampling frequency of Franfkurt, in the near future, more aircraft will join the IAGOS program, which may allow investigations of the diurnal ozone variations in other regions of the world.

References

Ayers GP, Penkett SA, Gillett RW, Bandy B, Galbally IE, et al. 1992. Evidence for photochemical control of ozone concentrations in unpolluted marine air. *Nature* **360**(6403): 446–449. doi: 10.1038/360446a0.

Balzani Lööv JM, Henne S, Legreid G, Staehelin J, Reimann S, et al. 2008. Estimation of background concentrations of trace gases at the Swiss Alpine site Jungfraujoch (3580 m asl). *J Geophys Res* **113**(D22): D22305. doi: 10.1029/2007JD009751.

Bedka KM. 2011. Overshooting cloud top detections using MSG SEVIRI Infrared brightness temperatures and their relationship to severe weather over Europe. *Atmos Res* **99**(2): 175–189. doi: 10.1016/j.atmosres.2010.10.001.

Bonasoni P, Stohl A, Cristofanelli P, Calzolari F, Colombo T, et al. 2000. Background ozone variations at Mt. Cimone Station. *Atmos Environ* **34**(29–30): 5183–5189. doi: 10.1016/S1352-2310(00)00268-5.

Brodin M, Helmig D, Oltmans S. 2010. Seasonal ozone behavior along an elevation gradient in the Colorado Front Range Mountains. *Atmos Environ* **44**(39): 5305–5315. doi: 10.1016/j.atmosenv.2010.06.033.

Brunner D, Staehelin J, Jeker D, Wernli H, Schumann U. 2001. Nitrogen oxides and ozone in the tropopause region of the northern hemisphere: Measurements from commercial aircraft in 1995/1996 and 1997. *J Geophys Res-Atmos* **106**(D21): 27673–27699. doi: 10.1029/2001JD900239.

Burley JD, Theiss S, Bytnerowicz A, Gertler A, Schilling S, et al. 2015. Surface ozone in the Lake Tahoe Basin. *Atmos Environ* **109**: 351–369. doi: 10.1016/j.atmosenv.2015.02.001.

Cooper OR, Eckhardt S, Crawford JH, Brown CC, Cohen RC, et al. 2009. Summertime buildup and decay of lightning NO_x and aged thunderstorm outflow above North America. *J Geophys Res* **114**(D1): D01101. doi: 10.1029/2008JD010293.

Cooper OR, Stohl A, Trainer M, Thompson AM, Witte JC, et al. 2006. Large upper tropospheric ozone enhancements above midlatitude North America during summer: In situ evidence from the IONS and MOZAIC ozone measurement network. *J Geophys Res* **111**(D24): D24S05. doi: 10.1029/2006JD007306.

Cooper OR, Trainer M, Thompson AM, Oltmans SJ, Tarasick DW, et al. 2007. Evidence for a recurring eastern North America upper tropospheric ozone maximum during summer. *J Geophys Res* **112**(D23): D23304. doi: 10.1029/2007JD008710.

Cristofanelli P, Fierli F, Marinoni A, Calzolari F, Duchi R, et al. 2013. Influence of biomass burning and anthropogenic emissions on ozone, carbon monoxide and black carbon at the Mt. Cimone GAW-WMO global station (Italy, 2165 m a.s.l.). *Atmos Chem Phys* **13**(1): 15–30. doi: 10.5194/acp-13-15-2013.

DeCaria AJ, Pickering KE, Stenchikov GL, Ott LE. 2005. Lightning-generated NO_x and its impact on tropospheric ozone production: A three-dimensional modeling study of a Stratosphere-Troposphere Experiment: Radiation, Aerosols and Ozone (STERAO-A) thunderstorm. *J Geophys Res Atmos* **110**(D14): 1–13. doi: 10.1029/2004JD005556.

Derwent R, Jenkin M, Saunders S, Pilling M, Simmonds P, et al. 2003. Photochemical ozone formation in north west Europe and its control. *Atmos Environ* **37**(14): 1983–1991. doi: 10.1016/S1352-2310(03)00031-1.

Emmons L, Carroll M, Hauglustaine D, Brasseur G, Atherton C, et al. 1997. Climatologies of NO_xx and NO_y: A comparison of data and models. *Atmos Environ* **31**(12): 1851–1904. doi: 10.1016/S1352-2310(96)00334-2.

Ezcurra A, Benech B, Echelecou A, Santamaría J, Herrero I, et al. 2013. Influence of local air flow regimes on the ozone content of two Pyrenean valleys. *Atmos Environ* **74**: 367–377. doi: 10.1016/j.atmosenv.2013.03.051.

Ganzeveld L, Helmig D, Fairall CW, Hare J, Pozzer A. 2009. Atmosphere-ocean ozone exchange: A global modeling study of biogeochemical, atmospheric, and waterside turbulence dependencies. *Global Biogeochem Cy* **23**(4): 1–16. doi: 10.1029/2008GB003301.

Helmig D, Tanner DM, Honrath RE, Owen RC, Parrish DD. 2008. Nonmethane hydrocarbons at Pico Mountain, Azores: 1. Oxidation chemistry in the North Atlantic region. *J Geophys Res* **113**(D20): D20S91. doi: 10.1029/2007JD008930.

Huntrieser H, Feigl C, Schlager H, Schröder F, Gerbig C, et al. 2002. Airborne measurements of NO_x, tracer species, and small particles during the European Lightning Nitrogen Oxides Experiment. *J Geophys Res Atmos* **107**(D11): ACH 5–1–ACH 5–24. doi: 10.1029/2000JD000209.

Huntrieser H, Schlager H, Feigl C, Höller H. 1998. Transport and production of NO_x in electrified thunderstorms: Survey of previous studies and new observations at midlatitudes. *J Geophys Res Atmos* **103**(D21): 28247–28264. doi: 10.1029/98JD02353.

Jonson JE, Simpson D, Fagerli H, Solberg S. 2006. Can we explain the trends in European ozone levels? *Atmos Chem Phys* **6**(1): 51–66. doi: 10.5194/acp-6-51-2006.

Marenco A, Thouret V, Nédélec P, Smit H, Helten M, et al. 1998. Measurement of ozone and water vapor by Airbus in-service aircraft: The MOZAIC airborne program, an overview. *J Geophys Res-Atmos* **103**(D19): 25631–25642. doi: 10.1029/98JD00977.

Monks PS. 2005. Gas-phase radical chemistry in the troposphere. *Chem Soc Rev* **34**(5): 376–395. doi: 10.1039/b307982c.

Monks PS, Archibald AT, Colette A, Cooper O, Coyle M, et al. 2015. Tropospheric ozone and its precursors from the urban to the global scale from air quality to short-lived climate forcer. *Atmos Chem Phys* **15**(15): 8889–8973. doi: 10.5194/acp-15-8889-2015.

Monks PS, Carpenter LJ, Penkett SA, Ayers GP, Gillett RW, et al. 1998. Fundamental ozone photochemistry in the remote marine boundary layer the soapex experiment, measurement and theory. *Atmos Environ* **32**(21): 3647–3664. doi: 10.1016/S1352-2310(98)00084-3.

Monks PS, Salisbury G, Holland G, Penkett SA, Ayers GP. 2000. A seasonal comparison of ozone photochemistry in the remote marine boundary layer. *Atmos Environ* **34**(16): 2547–2561. doi: 10.1016/S1352-2310(99)00504-X.

Nédélec P, Blot R, Boulanger D, Athier G, Cousin JM, et al. 2015. Instrumentation on commercial aircraft for monitoring the atmospheric composition on a global scale: The IAGOS system, technical overview of ozone and carbon monoxide measurements. *Tellus B* **67**: 1–16. doi: 10.3402/tellusb.v67.27791.

Oltmans S, Lefohn A, Shadwick D, Harris J, Scheel H, et al. 2013. Recent tropospheric ozone changes – A pattern dominated by slow or no growth. *Atmos Environ* **67**: 331–351. doi: 10.1016/j.atmosenv.2012.10.057.

Oltmans SJ, Komhyr WD. 1986. Surface ozone distributions and variations from 1973–1984: Measurements at the NOAA Geophysical Monitoring for Climatic Change Baseline Observatories. *J Geophys Res* **91**(D4): 5229–5236. doi: 10.1029/JD091iD04p05229.

Oltmans SJ, Levy II H. 1994. Surface ozone measurements from a global network. *Atmos Environ* **28**(1): 9–24. doi: 10.1016/1352-2310(94)90019-1.

Ordóñez C, Mathis H, Furger M, Henne S, Hüglin C, et al. 2005. Changes of daily surface ozone maxima in Switzerland in all seasons from 1992 to 2002 and discussion of summer 2003. *Atmos Chem Phys* **5**(5): 1187–1203. doi: 10.5194/acp-5-1187-2005.

Ott LE, Pickering KE, Stenchikov GL, Allen DJ, DeCaria AJ, et al. 2010. Production of lightning NO_x and its vertical distribution calculated from three-dimensional cloud-scale chemical transport model simulations. *J Geophys Res* **115**(D4): D04301. doi: 10.1029/2009JD011880.

Pan LL, Homeyer CR, Honomichl S, Ridley BA, Weisman M, et al. 2014. Thunderstorms enhance tropospheric ozone by wrapping and shedding stratospheric air. *Geophys Res Lett* **41**(22): 7785–7790. doi: 10.1002/2014GL061921.

Parrish DD, Law KS, Staehelin J, Derwent R, Cooper OR, et al. 2013. Lower tropospheric ozone at northern midlatitudes: Changing seasonal cycle. *Geophys Res Lett* **40**(8): 1631–1636. doi: 10.1002/grl.50303.

Petetin H, Thouret V, Fontaine A, Sauvage B, Athier G, et al. 2015. Characterizing tropospheric ozone and CO around Frankfurt between 1994–2012 based on MOZAIC-IAGOS aircraft measurements. *Atmos Chem Phys Discuss* **15**(17): 23841–23891. doi: 10.5194/acpd-15-23841-2015.

Petzold A, Thouret V, Gerbig C, Zahn A, Brenninkmeijer CAM, et al. 2015. Global-scale atmosphere monitoring by in-service aircraft – current achievements and future prospects of the European Research Infrastructure IAGOS. *Tellus B* **67**: 1–24. doi: 10.3402/tellusb.v67.28452.

Pryor S, Steyn D. 1995. Hebdomadal and diurnal cycles in ozone time series from the Lower Fraser Valley, B.C. *Atmos Environ* **29**(9): 1007–1019. doi: 10.1016/1352-2310(94)00365-R.

Ridley BA, Shetter JD, Gandrud BW, Salas LJ, Singh HB, et al. 1990. Ratios of peroxyacetyl nitrate to active nitrogen observed during aircraft flights over the eastern Pacific Oceans and continental United States. *J Geophys Res-Atmos* **95**(D7): 10179–10192. doi: 10.1029/JD095iD07p10179.

Ruxton GD. 2006. The unequal variance t-test is an underused alternative to student's t-test and the Mann-Whitney U test. *Behav Ecol* **17**(4): 688–690. doi: 10.1093/beheco/ark016.

Satterthwaite FE. 1946. An Approximate Distribution of Estimates of Variance Components. *Biometrics Bull* **2**(6): 110–114. doi: 10.2307/3002019.

Schumann U, Huntrieser H. 2007. The global lightning-induced nitrogen oxides source. *Atmos Chem Phys* **7**(14): 3823–3907. doi: 10.5194/acp-7-3823-2007.

Singh H, Chen Y, Tabazadeh A, Fukui Y, Bey I, et al. 2000. Distribution and fate of selected oxygenated organic species in the troposphere and lower stratosphere over the Atlantic. *J Geophys Res-Atmos* **105**(D3): 3795–3805. doi: 10.1029/1999JD900779.

Singh HB, Condon E, Vedder J, O'Hara D, Ridley BA, et al. 1990. Peroxyacetyl nitrate measurements during CITE 2: Atmospheric distribution and precursor relationships. *J Geophys Res Atmos* **95**(D7): 10163–10178. doi: 10.1029/JD095iD07p10163.

Singh HB, Ludwig FL, Johnson WB. 1978. Tropospheric ozone: Concentrations and variabilities in clean remote atmospheres. *Atmos Environ* **12**(11): 2185–2196. doi: 10.1016/0004-6981(78)90174-9.

Smith HF. 1936. The Problem of Comparing the Results of Two Experiments with Unequal Errors. *J Counc Sci Ind Res* **9**: 211–212.

Solberg S, Bergström R, Langner J, Laurila T, Lindskog A. 2005. Changes in Nordic surface ozone episodes due to European emission reductions in the 1990s. *Atmos Environ* **39**(1): 179–192. doi: 10.1016/j.atmosenv.2004.08.049.

Solberg S, Hov Ø, Søvde A, Isaksen ISA, Coddeville P, et al. 2008. European surface ozone in the extreme summer 2003. *J Geophys Res* **113**(D7): D07307. doi: 10.1029/2007JD009098.

Thouret V, Cammas JP, Sauvage B, Athier G, Zbinden R, et al. 2006. Tropopause referenced ozone climatology and inter-annual variability (1994–2003) from the MOZAIC programme. *Atmos Chem Phys* **6**(4): 1033–1051. doi: 10.5194/acp-6-1033-2006.

Thouret V, Marenco A, Logan JA, Nédélec P, Grouhel C. 1998. Comparisons of ozone measurements from the MOZAIC airborne program and the ozone sounding network at eight locations. *J Geophys Res* **103**(D19): 25695–25720. doi: 10.1029/98JD02243.

Tressol M, Ordonez C, Zbinden R, Brioude J, Thouret V, et al. 2008. Air pollution during the 2003 European heat wave as seen by MOZAIC airliners. *Atmos Chem Phys* **8**(8): 2133–2150. doi: 10.5194/acp-8-2133-2008.

Wapler K. 2013. High-resolution climatology of lightning characteristics within Central Europe. *Meteorol Atmos Phys* **122**(3–4): 175–184. doi: 10.1007/s00703-013-0285-1.

Welch BL. 1938. The Significance of the Difference Between Two Means When the Population Variances are Unequal. *Biometrika* **29**(3/4): 350–362. doi: 10.2307/2332010.

Zbinden RM, Cammas JP, Thouret V, Nédélec P, Karcher F, et al. 2006. Mid-latitude tropospheric ozone columns from the MOZAIC program: Climatology and interannual variability. *Atmos Chem Phys* **6**(4): 1053–1073. doi: 10.5194/acp-6-1053-2006.

Zhang J, Rao ST. 1999. The Role of Vertical Mixing in the Temporal Evolution of Ground-Level Ozone Concentrations. *J Appl Meteorol* **38**(12): 1674–1691. doi: 10.1175/1520-0450(1999)038<1674:TROVMI>2.0.CO;2.

Zhang L, Jacob DJ, Kopacz M, Henze DK, Singh K, et al. 2009. Intercontinental source attribution of ozone pollution at western U.S. sites using an adjoint method. *Geophys Res Lett* **36**(11): L11810. doi: 10.1029/2009GL037950.

Zhang L, Jin L, Zhao T, Yin Y, Zhu B, et al. 2015. Diurnal variation of surface ozone in mountainous areas: Case study of Mt. Huang, East China. *Sci Total Environ* **538**: 583–590. doi: 10.1016/j.scitotenv.2015.08.096.

Zhang R, Lei W, Tie X, Hess P. 2004. Industrial emissions cause extreme urban ozone diurnal variability. *P Natl Acad Sci* **101**(17): 6346–6350. doi: 10.1073/pnas.0401484101.

Contributions

- Contributed to conception and design: HP, OC
- Contributed to acquisition of data: HP, VT, GA, RB, DB, J-MC, PN
- Contributed to analysis and interpretation of data: HP, VT, AG, OC
- Drafted and/or revised the article: HP
- Approved the submitted version for publication: HP, VT, GA, RB, DB, J-MC, AG, PN, OC

Acknowledgments

The authors acknowledge the strong support of the European Commission, Airbus, and the Airlines (Lufthansa, Air-France, Austrian, Air Namibia, Cathay Pacific, Iberia and China Airlines so far) who carry the MOZAIC or IAGOS equipment and perform the maintenance since 1994. In its last 10 years of operation, MOZAIC has been funded by INSU-CNRS (France), Météo-France, Université Paul Sabatier (Toulouse, France) and Research Center Jülich (FZJ, Jülich, Germany). IAGOS has been additionally funded by the EU projects IAGOS-DS and IAGOS-ERI. The MOZAIC-IAGOS database is supported by ETHER (CNES and INSU-CNRS). Data are also available via Ether web site www.pole-ether.fr. The authors are also grateful to the Air Monitoring Network of the Federal Environment Agency of Germany for providing the O_3 measurements at the Rannheim, Darmstadt, Spessart and Waldhof monitoring sites, and to the Global Atmosphere Watch (GAW) program for hosting and delivering the Waldhof data.

Funding information

Owen Cooper and Audrey Gaudel are funded by NOAA's Health of the Atmosphere and Atmospheric Chemistry and Climate Programs.

Competing interests

The authors have declared that no competing interests exist.

Data accessibility statement

No new measurements were made for this review article. All ozone datasets mentioned in the text were obtained from existing databases. The MOZAIC-IAGOS data are available on http://www.iagos.fr. The O_3 observations at surface stations around Frankfurt are available on request from the German Federal Environment Agency (Umweltbundesamt, UBA; contact immission@uba.de).

Supplemental material

- **Table S1. Total number of O_3 observations over the 1994–2012 period. (DOC)**
  Results are given per pressure level and per 3-hour time period. The 0–3 UTC time period is ignored due to too sparse data. The largest number of data are found at 3–6, 6–9 and 9–12 UTC, with more than 1.2 millions observations along the tropospheric column. This number is reduced to about 0.8 million at 12–15 UTC, and below 0.5 million during the other time periods. Data are the sparsest at 18–21 UTC with about 0.2 million observations along the tropospheric column.
- **Figure S1. Influence of the sub-sampling related to the MOZAIC-IAGOS dataset. (PDF)**
  The diurnal variations of mean O_3 mixing ratios are calculated at several surface stations around Frankfurt (see text in Sect. 2.3 for details on these stations), both at the seasonal and annual scale (DJF: winter, MAM: spring, JJA: summer, SON: autumn, ANN: annual). The REF diurnal cycles (in black) represent the true diurnal cycles obtained at the surface when considering all the data available between 1994 and 2012. The SUB1 diurnal cycles (in red) represent the diurnal cycles obtained when considering only the months with at least one MOZAIC-IAGOS observation at 1000 hPa at Frankfurt at a given pressure level and season. Similarly, the SUB50 diurnal cycles (in green) correspond to the diurnal cycles based on months with at least 50 MOZAIC-IAGOS observations at Frankfurt. Except for the 0–3 UTC time interval that is ignored in our study, the different diurnal cycles are very similar.
- **Figure S2. Diurnal variations of several O_3 percentiles in the troposphere above Frankfurt, in winter (DJF). (PDF)**
  Results are shown for the O_3 5th, 25th, 50th, 75th and 95th percentiles. Diurnal variations are slightly more noisy than at the annual scale (see Fig. 3), likely due to the lower number of points considered. These noisy variations are higher during the second half of the day (in particular for the 5th and 95th percentiles) when less data are available.
- **Figure S3. Same as in Fig. S2 but for spring (MAM). (PDF)**
- **Figure S4. Same as in Fig. S2 but for summer (JJA). (PDF)**
- **Figure S5. Same as in Fig. S2 but for autumn (SON). (PDF)**
- **Figure S6. Changes of the O_3 diurnal variations between 1994–2003 and 2004–2012 in winter (DJF). (PDF)**
  Diurnal profiles of mean tropospheric O_3 mixing ratios are given for 1994–2003 (left panel) and 2004–2012 (middle panel). The relative differences of mixing ratio between the two periods are shown in the right panel. Crosses indicate the pressure levels and time interval at which the differences are statistically significant regarding the SWS t-test (see text in Sect. 3.1 for details on this test). The increase of O_3 mixing ratios is the strongest during winter, in particular close to the surface where changes exceed +20% while changes range between +5 and +15% higher in altitude during most of the day.
- **Figure S7. Same as Fig. S6 in spring (MAM). (PDF)**
  Compared to winter (see Fig. S6), the changes of O_3 mixing ratios between 1994–2003 and 2004–2012 are weaker in spring, with values ranging between -5 and +10% in most of the troposphere (except in the first pressure level where the increase remain above +20% during the night).

Diurnal cycle of ozone throughout the troposphere

- **Figure S8. Same as in Fig. S6 but for summer (JJA). (PDF)**
  Contrary to the other seasons, results in summer show substantially lower O_3 mixing ratios in 2004–2012 than in 1994–2003 below 700 hPa (again except in the first pressure level during the night), with changes up to -15 and -20%, in particular during the middle of the day.
- **Figure S9. Same as in Fig. S6 but for autumn (SON). (PDF)**
  The changes of O_3 mixing ratios in autumn show an increase below 700 hPa during most of the day (except at 15–18 UTC when mixing ratios are shown to increase), although changes all remain below ±20%.
- **Figure S10. Changes of the diurnal variations of the O_3 5th percentile at the annual scale (ANN). (PDF)**
  As for the previous figures, diurnal profiles are shown for 1994–2003 (left panel) and 2004–2012 (middle panel), while the relative differences of mixing ratios between the two periods is shown in the right panel. Compared to the changes of the mean O_3 mixing ratios (see Fig. 5), the increase of the O_3 5th percentile appears stronger, with changes above +15% in a large part of the troposphere, in particular below 700 hPa. The changes are reduced higher in altitude.
- **Figure S11. Same as in Fig. S10 but for the O_3 95thpercentile. (PDF)**
  Contrary to the O_3 5th percentile previously described in Fig. S10, results here indicate a decrease of the O_3 95th percentile at the annual scale between -5 and -15% below 700 hPa, mostly during the middle of the day. The picture is more contrasted higher in altitude where changes range between -10 and +10%.